Integration preconditioning for ocean bottom node data

Arash JafarGandomi, Amarjeet Kumar, Sergio Grion (Shearwater Geoservices)

Summary

We investigate options to perform integration preconditioning for Ocean bottom node (OBN) data acquired with accelerometers. When amplitude perturbations due to sensor saturation are present, integration exaggerates them through convolution with the integration filter; therefore, their correction is desirable. Furthermore, the affected samples may impact PZ calibration, wavefield separation and multi-dimensional deconvolution, therefore a high fidelity correction is needed. We found that two algorithms, a 5D version of POCS (Projection into Convex Sets) and an adaptive version of PINNs (Physics Informed Neural Networks) are effective at interpolating the few affected data samples. We present examples of their application to field data acquired with either a standard source array or a bandwidth-controlled source array, as the latter reduces sensor saturation and complements the proposed processing solution.

Introduction

The acquisition of multicomponent seismic data on the ocean bottom is common practice. In shallow water, the source can be very close to the seabed receiver and the amplitude of the seismic signal arriving may exceed the dynamic range of the recording sensor. For Ocean Bottom Nodes (OBN), the direct arrival on the hydrophone and occasionally on the vertical component recording may be clipped. This issue affects all types of recording sensors on the seabed, including hydrophones, geophones, DAS cables (Distributed Acoustic Sensing) and MEMS (Micro-Electro-Mechanical Systems).

Recently MEMS-based particle acceleration measurements entered the commercial marine seismic market. These were first introduced in streamers (Paulson et. al, 2015) and later in OBN (Hager, et. al, 2022, Tellier et. al, 2023). The flat and undistorted amplitude and phase spectrum of MEMS sensors over the entire desired bandwidth, extending down to 0 Hz, provides the highest signal fidelity. Additionally, these sensors allow for the real-time extraction of pitch and roll information directly from the sensor itself, eliminating the need for separate measurements.

Rentsch et al. (2025, submitted for the EAGE annual conference) highlight that source energy beyond the seismic bandwidth can cause saturation, and a saturated MEMS may clip cleanly or experience a very short temporary loss of its force feedback control loop (often referred to as overdrive), leading to amplitude perturbations in the near offsets. However, Rentsch et al. 2025 show that the onset of saturation and overdrive can be effectively delayed through the use of bandwidth-controlled seismic sources, such as eSource and Bluepulse. As a reference on bandwidth-controlled sources, see for example Laws (2013). When amplitude perturbations are present on acceleration data, the subsequent integration to velocity required for multicomponent wavefield separation will be affected by leaving an imprint of the integration filter.

In this study we investigate the processing solution for saturation and overdrive. We propose effective approaches for correcting affected samples as a preconditioning to integration as well as for general use in the presence of clipping for any component. This step should be performed before multicomponent data rotation to limit its application to those components affected during acquisition.

The affected samples are usually of the order of few milliseconds even in extreme cases. We found that interpolation approaches can solve this problem. It should be noted that the problem at hand is different from the classic interpolation problem that applies to whole traces, as only a few samples are at play here.

Previous studies have explored the use of Projection Onto Convex Sets (POCS), initially proposed by Abma and Kabir (2006), for reconstructing overdriven samples in 1D (Zhang et al., 2016) and 2D (Seher, 2024) Fourier domains. Building on these methods, we present two approaches: the use of an adaptive version of Physics-Informed Neural Networks (PINNs) and the extension of POCS to multi-dimensional domains. These approaches are demonstrated with both synthetic and real data examples.

PINNslope interpolation

Recently Brandolin et al. (2023) introduced PINNslope, a seismic data interpolation method utilizing PINNs as described by Raissi et al. (2019). This innovative framework interpolates seismic data while simultaneously estimating the local slope field by jointly training two feed-forward neural networks.

The training leverages both the local plane-wave partial differential equation (PDE) and the available observed data, incorporating them as distinct terms in the loss function. Despite the promising results, a significant hurdle of this technology is its slow learning process, requiring numerous iterations to achieve an acceptable reconstructed result. Kumar & JafarGandomi (2024) addressed this challenge by introducing an adaptive step in this approach. The improved method dynamically adjusts both the linear layers and the activation functions of the network architecture, which in turn not only enhances the accuracy of the reconstructed wavefields but also substantially reduces the number of training epochs required.

This methodology takes input data (d_j), identifies traces or samples for reconstruction, and uses PINNslope with two parallel neural networks to update the wavefield (u_j) and estimate slopes (σ^+ & σ^-). The loss function (J) includes three terms: two enforcing physics-based constraints via plane wave PDEs (one with a positive slope σ^+ and the other with a negative slope σ^-) and one minimizing data loss at known locations:

$$J = \lambda\left(\frac{1}{N_t}\sum_{j=0}^{N_t}\left|d_j - u_j\right|\right) + \frac{1}{N_u}\sum_{i=0}^{N_u}\left(\frac{\partial u_i}{\partial x} + \sigma^+\frac{u_i}{\partial t}\right) + \frac{1}{N_u}\sum_{i=0}^{N_u}\left(\frac{\partial u_i}{\partial x} + \sigma^-\frac{u_i}{\partial t}\right) \quad (1)$$

where, N_t are the number of known grid point locations and N_u are the total number of grid point locations. The scalar λ is the weighting parameter controlling the influence of the data term. To accelerate results, we use adaptive linear layers followed by adaptive activation functions.

As explained by Kumar & JafarGandomi (2024), the main innovative steps we use to achieve significant speedup involve incorporating adaptive linear layers and adaptive activation functions into the network architecture (Cortes, 2016). The linear layers are transformed by incorporating a learnable scaler, denoted as α, to dynamically adjust the outputs, making the linear transformation $\boldsymbol{y} = \boldsymbol{\alpha}(\boldsymbol{Wx} + \boldsymbol{b})$, where $\boldsymbol{W}$ and $\boldsymbol{b}$ are weights and biases of each neuron in the network. This adaptation allows the network to fine-tune the influence of each layer, providing greater flexibility and control over the learning process.

Additionally, we enhance the robustness of the activation functions by implementing adaptive activation with shifting. Specifically, we introduce learnable parameters $\boldsymbol{\alpha}$ and $\boldsymbol{\beta}$ into the activation function, modifying it to $\boldsymbol{\alpha}(\boldsymbol{Tanh} * \boldsymbol{x} + \boldsymbol{\beta})$. This adjustment allows the network to dynamically modify both the amplitude and the shift of the activation function, making it more adaptable to the varying scales and shifts in the data. This dual adaptation strategy significantly accelerates the convergence of the PINNs, leading to more efficient and effective learning of complex physical patterns. The adaptive nature of $\boldsymbol{\alpha}$ and $\boldsymbol{\beta}$ ensures their continual adjustment based on training data, contributing to faster training processes. Through our experiments, we have observed that results which previously required 15,000 epochs without adaptive methods, can now be achieved in just 1,500 epochs with adaptive techniques.

Multidimensional POCS interpolation

POCS (Abma and Kabir, 2006) is a well-known approach for reconstructing missing data in the seismic industry. This technique is based on the principle of projecting data onto a set of convex constraints, which represent the known properties of the data. The POCS method iteratively refines the data by alternating between the time-space domain and a transform domain, such as the Fourier domain.

Due to its computational cost, POCS is usually limited to one or two dimensions. To ensure the fidelity of the reconstructed amplitudes, we extended the approach to five dimensions by using multiple sources and receivers simultaneously using a 5D frequency-wavenumber transform. This approach is computationally affordable because for our integration preconditioning application we are only interested in reconstructing a very small portion of the data in both space and time.

Other possible approaches

During our research, we explored a method involving de-ghosting and re-ghosting the pressure component to calculate a simulated vertical component and hence a correction factor for anomalous amplitudes on real vertical component. However, this approach proved ineffective due to several challenges: the difficulty in parameterizing the ghost operator, the presence of aliasing, and the need to accurately separate the direct arrival from the seabed reflection.

We also considered calculating the correction factor specifically for data between the direct arrival and the first-order multiple, leveraging the one-way nature of the wavefield in this zone. This method allows for the straightforward calculation of particle velocity or acceleration from pressure based on Newton's law. However, it also requires the separation of the direct arrival and, besides, becomes unreliable in very shallow water. Consequently, we abandoned these two approaches and focused on the POCS and PINNs methods described earlier.

Detection of perturbed amplitudes

The first step in the reconstruction of anomalous amplitudes is their detection. In the case of MEMS the vertical component, bearing the maximum of the gravity component (up to 1g depending on orientation), is usually more exposed than horizontal components. Modelling studies and field observations indicate the maximum offset range for detection. Within this offset range, detection is performed using the velocity domain, where acceleration anomalies are more evident because of the imprint of the integration filter.

The method identifies perturbed amplitudes in seismic data by analysing trace signals through integration, filtering, differentiation, and thresholding. The acceleration data in gravitational units (g) are integrated to obtain velocity, and the resulting signal is smoothed with a median filter to eliminate noise. Following this, the derivative of the smoothed velocity signal is calculated to highlight rapid amplitude variations. A threshold is applied to this derivative to detect regions where the amplitude surpasses a predefined limit, marking them as anomalies. This procedure helps pinpoint the sample range that requires reconstruction using the methods mentioned above (PINNs or 5D POCS).

Examples

The data examples come from a 2D OBN test line acquired in the North Sea. The water depth is 100m. The receiver line is 2km long, with OBNs 50m apart. The source line is 6.5km long, with 25m flip-flop shooting and 50m cross-line separation between the sources, so that the shot points are at 25m cross-line from the receiver line. The source line operated 3147in^3 arrays: a standard array and a bandwidth-controlled array were used at alternating shot points.

Figures 1a and 1e show the raw vertical components of the acceleration records and the particle velocity components of a common-receiver gather obtained by numerical integration of the recorded MEMS data for the standard source. Corresponding records from the bandwidth-controlled source are shown in Figures 1b and 1f, respectively. Note that for the data acquired with the standard source small perturbations are present at the near offsets right after the direct arrival. The duration of these perturbations is about 20ms. These perturbations become more noticeable in the integrated domain (Fig 1e). Such perturbation is not observed for the bandwidth-controlled source. In order to avoid the artefacts in the integrated domain, we first detected and removed the affected samples (as discussed above) and then tested both reconstruction approaches, POCS and PINNs. The reconstruction results are shown in Figures 1c and 1d, and the corresponding integrated records in Figures 1g and 1h for POCS and PINNs, respectively. Both reconstruction results are satisfactory in both the acceleration and particle velocity domains, but blind test benchmarks show that the PINNs method performs better in terms of precision. Synthetic studies and other tests performed on real data also confirm that the PINNs method in general performs better, although at a higher computational cost.

Occasionally several neighboring traces may suffer from this amplitude perturbation effect. To better demonstrate this Figure 2 shows a common-shot gather where five traces have been affected. The arrangement of the panels in this figure is the same as those in Figure one and the same conclusions can be drawn in terms of successful preconditioning, and improved results with PINNs over POCS.

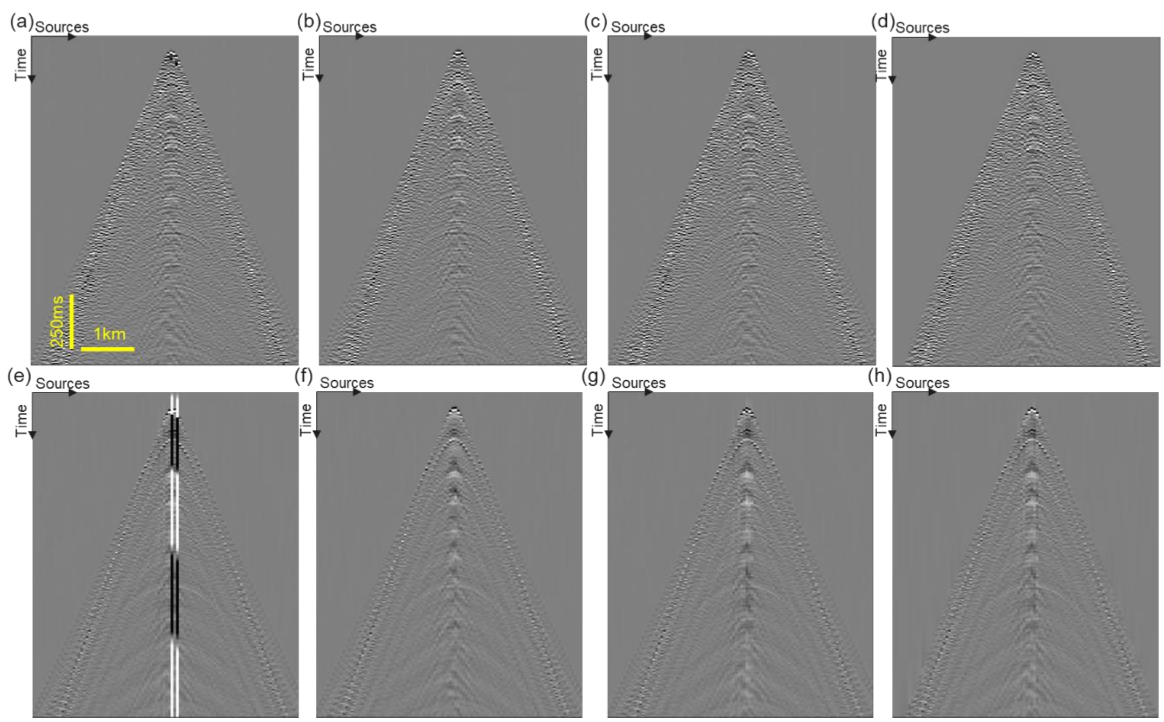

Figure 1: (a & b) A common-receiver gather showing measured vertical component acceleration with standard source and bandwidth controlled source, respectively, c) precondition of a) with POCS and d) with PINNs. The bottom row (e-h) shows the corresponding images after integration into the particle velocity domain.

Discussions

While PINNs have demonstrated their potential for solving interpolation problems with embedded partial differential equations constraints, their practical application to large-scale seismic interpolation remains challenging. Our study highlights the effectiveness of POCS for reconstruction, particularly when applied across the entire dataset.

One of the key challenges with PINNs is their sensitivity to random initialization, where different random seeds can lead to variations in the results, often necessitating multiple runs to achieve consistency. Additionally, the computational cost of training PINNs is significantly higher than that of traditional methods, requiring GPUs and substantial processing power. The training process is inherently slow, often demanding numerous iterations to achieve convergence, even with adaptive optimization techniques. As a result, PINNs are typically applied in 2D space, whereas POCS can efficiently operate in 5D space at a much lower computational cost.

These limitations emphasize the need for further research to enhance the training stability, computational efficiency, and scalability of PINNs to higher-dimensional problems. Addressing these challenges is an ongoing effort, and we aim to explore potential improvements in future work, providing updates in subsequent publications.

Conclusions

We investigated several options for integration preconditioning of OBN data acquired with accelerometers and focused on two interpolation-based approaches to remove anomalous amplitudes: Physics Informed Neural Networks (PINNs) and 5D POCS (Projection into Convex Sets).

Interpolation proved effective, as the number of affected samples is small. This fact along with the high precision of these algorithms, compensates for the known difficulty of interpolating high-frequency, shallow data. We found that both methods are effective, with the first delivering greater accuracy at the expense of a higher computational cost. We demonstrated both methods on a field data example acquired using an OBN equipped with a hydrophone and MEMS accelerometers and both a standard 3147in^3 source and a bandwidth-controlled source of the same volume.

Acknowledgements

The authors also wish to acknowledge Shearwater GeoServices for permission to publish this work.

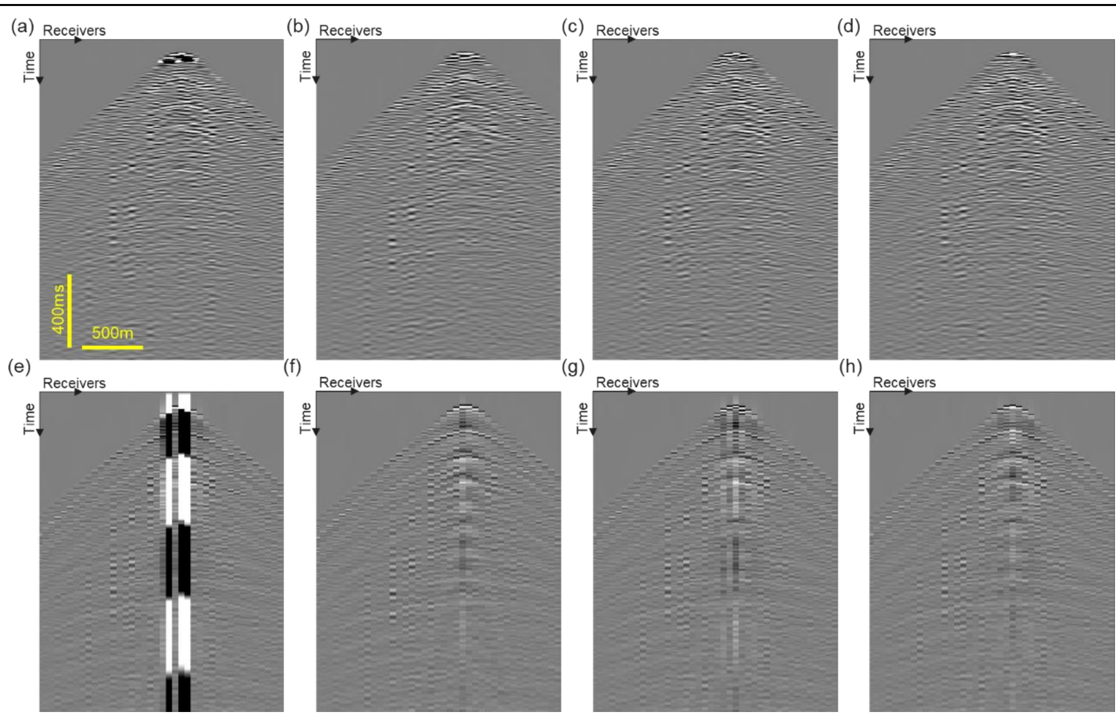

Figure 2: (a & b) A common-shot gather showing measured vertical component acceleration with standard source and bandwidth controlled source, respectively, c) precondition of a) with POCS and d) with PINNs. The bottom row (e-h) shows the corresponding images after integration into the particle velocity domain.